Acta Crystallographica Section B
Structural Science
ISSN 0108-7681

Anhydrous *versus* hydrated N^4-substituted 1*H*-pyrazolo[3,4-*d*]pyrimidine-4,6-diamines: hydrogen bonding in two and three dimensions

Jorge Trilleras,[a] Jairo Quiroga,[a] Justo Cobo,[b] Antonio Marchal,[b] Manuel Nogueras,[b] John N. Low[c] and Christopher Glidewell[d]*

[a]Grupo de Investigación de Compuestos Heterocíclicos, Departamento de Química, Universidad de Valle, AA 25360 Cali, Colombia, [b]Departamento de Química Inorgánica y Orgánica, Universidad de Jaén, 23071 Jaén, Spain, [c]Department of Chemistry, University of Aberdeen, Meston Walk, Old Aberdeen AB24 3UE, Scotland, and [d]School of Chemistry, University of St Andrews, St Andrews, Fife KY16 9ST, Scotland

Correspondence e-mail: cg@st-andrews.ac.uk

Received 22 April 2008
Accepted 30 June 2008

Ten new N^4-substituted 1*H*-pyrazolo[3,4-*d*]pyrimidine-4,6-diamines have been synthesized and the structures of nine of them are reported here, falling into two clear groups, those which are stoichiometric hydrates and those which crystallize in solvent-free forms. In each of N^4-methyl-N^4-phenyl-1*H*-pyrazolo[3,4-*d*]pyrimidine-4,6-diamine, $C_{12}H_{12}N_6$ (I), N^4-cyclohexyl-N^4-methyl-1*H*-pyrazolo[3,4-*d*]pyrimidine-4,6-diamine, $C_{12}H_{18}N_6$ (II), and N^4-(3-chlorophenyl)-1*H*-pyrazolo[3,4-*d*]pyrimidine-4,6-diamine, $C_{11}H_9ClN_6$ (III), the molecules are linked into hydrogen-bonded sheets. The molecules of 2-{4-(6-amino-1*H*-pyrazolo[3,4-*d*]pyri-]pyrimidin-4-yl)piperazin-1-yl}ethanol, $C_{11}H_{17}N_7O$ (IV), are linked into a three-dimensional framework, while the structure of N^4-methyl-N^4-(4-methylphenyl)-1*H*-pyrazolo-[3,4-*d*]pyrimidine-4,6-diamine monohydrate, $C_{13}H_{14}N_6\cdot H_2O$ (V), is only two-dimensional despite the presence of five independent hydrogen bonds. The stoichiometric hemihydrates N^4-ethyl-N^4-phenyl-1*H*-pyrazolo[3,4-*d*]pyrimidine-4,6-diamine hemihydrate, $C_{13}H_{14}N_6\cdot 0.5H_2O$ (VI) and N^4-(4-methoxyphenyl)-N^4-methyl-1*H*-pyrazolo[3,4-*d*]pyrimidine-4,6-diamine hemihydrate, $C_{13}H_{14}N_6O\cdot 0.5H_2O$ (VII), exhibit remarkably similar sheet structures, despite different space groups and Z' values, $Z' = 0.5$ in $C2/c$ for (VI) and $Z' = 1$ in $P\bar{1}$ for (VII). N^4-4-Benzyl-N^4-phenyl-1*H*-pyrazolo[3,4-*d*]pyrimidine-4,6-diamine monohydrate, $C_{18}H_{16}N_6\cdot H_2O$ (VIII), crystallizes with $Z' = 2$ in $P2_1/n$, and the four independent molecular components are linked into sheets by a total of 11 intermolecular hydrogen bonds. The sheet structure in {4-(pyrrolidin-1-yl)-1*H*-pyrazolo[3,4-*d*]pyrimi-]pyrimidine-6-amine} ethanol hemisolvate hemihydrate, $C_9H_{12}N_6\cdot 0.5C_2H_6O\cdot 0.5H_2O$ (IX), is built from the pyrimidine and water components only; it contains eight independent hydrogen bonds, and it very closely mimics the sheets in (VI) and (VII); the ethanol molecules are pendent from these sheets. The N^4-alkyl-N^4-aryl-4-aminopyrazolopyrimidine molecules in (I), (V)–(VIII) all adopt very similar conformations, dominated in each case by an intramolecular C—H$\cdots\pi$(arene) hydrogen bond: this interaction is absent from (III) where the molecular conformation is entirely different and probably dominated by the intermolecular hydrogen bonds.

1. Introduction

Pyrazolopyrimidines are isoelectronic and isosteric with purines and they exhibit a number of useful properties as antimetabolites in purine biochemical reactions. Pyrazolo[1,5-*a*]pyrimidines, for example, are of interest because of their antitrypanosomal (Novinson *et al.*, 1976) and antischistosomal (Senga *et al.*, 1981) activities, while pyrazolo[3,4-*b*]pyrimidines

exhibit antiviral properties (Moukha-Chafiq *et al.*, 2006), as well as finding uses in the treatment of immunological, inflammatory and proliferative diseases (Rice *et al.*, 2006). In parallel with a programme for the development of new synthetic approaches to these valuable ring systems, we have undertaken a programme of structural investigation and we have found in the pyrazolo[1,5-*a*]pyrimidine series that comparatively modest variations in the molecular constitutions of such pyrazolopyrimidines can induce substantial changes in the crystal structures, in particular in their crystallization characteristics and patterns of supramolecular aggregation (Portilla *et al.*, 2005, 2007; Portilla, Quiroga, Cobo *et al.*, 2006; Portilla, Quiroga, de la Torre *et al.*, 2006).

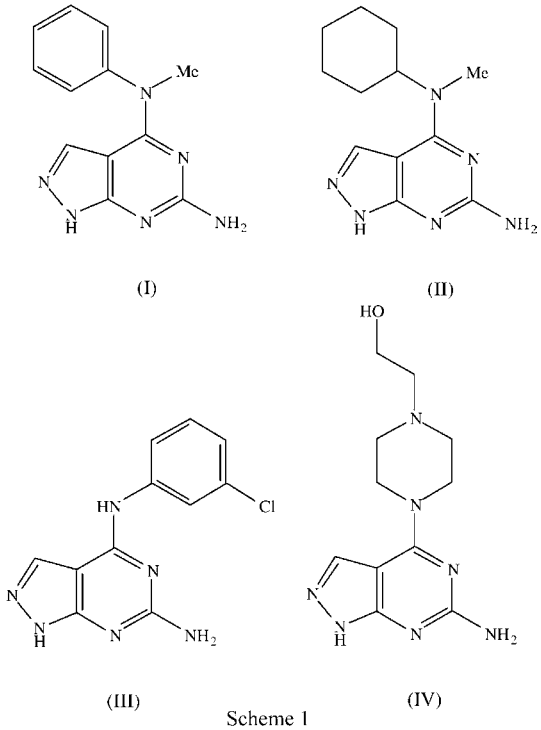

Scheme 1

In view of the wide structural diversity induced by small changes in molecular constitution in pyrazolo[1,5-*a*]-pyrimidines, we have now extended this structural study to a series of closely related pyrazolo[3,4-*d*]pyrimidines, where the heterocyclic nucleus is a simple isomer of that in purines, involving just a simple pairwise exchange of one C atom with one N atom in the five-membered ring. Compounds (I)–(IV) (Scheme 1), all crystallize from laboratory ethanol in solvent-free form, and (V)–(IX) (Scheme 2), all crystallize as stoichiometric solvates, mainly as simple hydrates, although the crystals of (IX) contain both water and ethanol of solvation. While a number of structures have been reported for compounds containing the pyrazolo[3,4-*d*]pyrimidine fragment, the majority of them, particularly in the work of Seela and his colleagues (Seela *et al.*, 1999, 2000; He *et al.*, 2002; Lin *et al.*, 2005; Seela, Jawalekar *et al.*, 2005; Seela, Sirivolu *et al.*, 2005; Seela, Zhang *et al.*, 2005; Zhang *et al.*, 2006), as well as that of others (Biswas *et al.*, 1996; Larson *et al.*, 1988), concern synthetic nucleoside analogues, often carrying a ribose-derived substituent on the N1 atom of the pyrazole ring, while the free amino group analogous to that at C6 in (I)–(IX) reported here is absent. As in most other reported metal-free analogues the N1 atom is substituted, while the free amino group is absent (Maulik *et al.*, 2000; Avasthi, Rawat, Chandra *et al.*, 2002; Avasthi, Rawat, Sarkhel *et al.*, 2002; Avasthi, Tewari *et al.*, 2002; Avasthi, Bal *et al.*, 2003; Avasthi, Bhagat *et al.*, 2003; Avasthi, Farooq *et al.*, 2003). Accordingly, the supramolecular aggregation patterns in examples of these types bear no resemblance to those in the structures reported here.

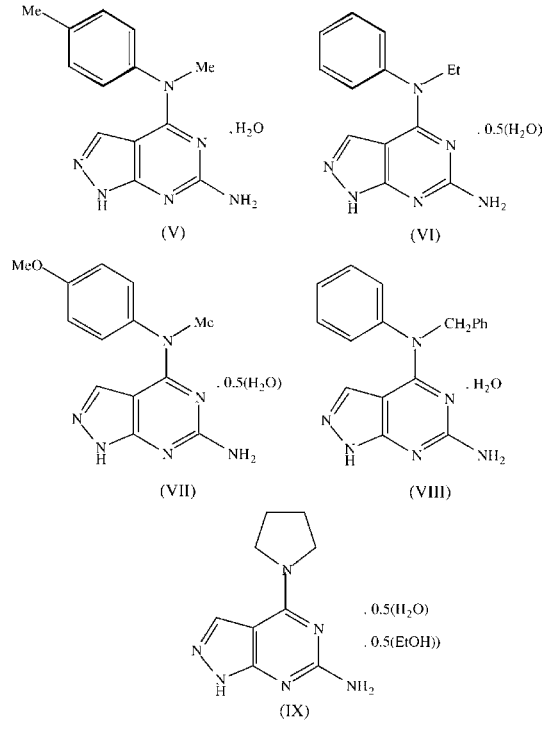

Scheme 2

Compounds (I)–(IX) were all prepared by reaction of an appropriately N^4-substituted 2,4-diamino-6-chloro-5-formylpyrimidine with aqueous hydrazine (Scheme 3), and all can be prepared by this method either by conducting the reactions in boiling ethanol (Bouder & Knochel, 2006) or, using 'green-chemistry' methods, in solvent-free reactions under brief microwave irradiation. Use of identical crystallization conditions yielded (I)–(IV) in anhydrous form, while (V)–(IX) all formed stoichiometric monohydrates [(V) and (VIII)] or hemihydrates [(VI), (VII) and (IX)].

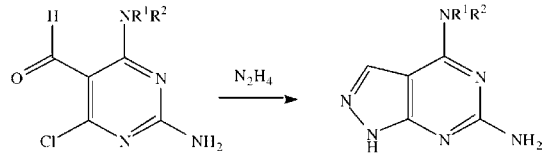

Scheme 3

2. Experimental

2.1. Syntheses

Compounds (I)–(IX) were prepared by reaction of the corresponding N^4-substituted 2-amino-6-chloro-5-formylpyr-

Table 1
Experimental details.

	(I)	(II)	(III)	(IV)	(V)
Crystal data					
Chemical formula	$C_{12}H_{12}N_6$	$C_{12}H_{18}N_6$	$C_{11}H_9ClN_6$	$C_{11}H_{17}N_7O$	$C_{13}H_{14}N_6\cdot H_2O$
M_r	240.28	246.33	260.69	263.32	272.32
Cell setting, space group	Monoclinic, $P2_1/n$	Monoclinic, $P2_1/n$	Monoclinic, $P2_1/c$	Orthorhombic, *Pbca*	Orthorhombic, *Pbca*
Temperature (K)	120 (2)	120 (2)	120 (2)	120 (2)	120 (2)
a, b, c (Å)	10.6661 (12), 7.7279 (9), 14.359 (2)	11.2407 (10), 7.3654 (5), 15.8178 (12)	11.1960 (8), 8.5040 (8), 13.3815 (12)	7.0297 (9), 13.859 (3), 25.766 (6)	16.5577 (12), 8.6833 (3), 18.4640 (13)
β (°)	100.071 (7)	106.005 (7)	120.674 (5)	90.00	90.00
V (Å^3)	1165.3 (3)	1258.83 (17)	1095.80 (16)	2510.2 (9)	2654.7 (3)
Z	4	4	4	8	8
D_x (Mg m^{-3})	1.369	1.300	1.580	1.393	1.363
Radiation type	Mo $K\alpha$	Mo $K\alpha$	Mo $K\alpha$	Mo $K\alpha$	Mo $K\alpha$
μ (mm^{-1})	0.09	0.09	0.34	0.10	0.09
Crystal form, colour	Block, colourless	Block, colourless	Lath, colourless	Lath, colourless	Block, colourless
Crystal size (mm)	0.58 × 0.41 × 0.34	0.32 × 0.28 × 0.18	0.55 × 0.21 × 0.10	0.20 × 0.10 × 0.08	0.37 × 0.24 × 0.23
Data collection					
Diffractometer	Bruker–Nonius KappaCCD	Bruker–Nonius KappaCCD	Bruker–Nonius KappaCCD	Bruker–Nonius KappaCCD	Bruker–Nonius KappaCCD
Data collection method	φ and ω scans	φ and ω scans	φ and ω scans	φ and ω scans	φ and ω scans
Absorption correction	Multi-scan	Multi-scan	Multi-scan	Multi-scan	Multi-scan
T_{min}	0.953	0.964	0.836	0.985	0.969
T_{max}	0.970	0.985	0.967	0.992	0.979
No. of measured, independent and observed reflections	27 117, 2674, 1737	32 264, 2885, 1763	26 526, 2515, 1452	59 170, 2877, 1479	61 337, 3046, 2146
Criterion for observed reflections	$I > 2\sigma(I)$	$I > 2\sigma(I)$	$I > 2\sigma(I)$	$I > 2\sigma(I)$	$I > 2\sigma(I)$
R_{int}	0.054	0.110	0.108	0.171	0.066
θ_{max} (°)	27.5	27.5	27.5	27.5	27.5
Refinement					
Refinement on	F^2	F^2	F^2	F^2	F^2
$R[F^2 > 2\sigma(F^2)]$, $wR(F^2)$, S	0.056, 0.169, 1.10	0.061, 0.142, 1.06	0.060, 0.183, 1.06	0.071, 0.224, 1.01	0.047, 0.122, 1.09
No. of reflections	2674	2885	2515	2877	3046
No. of parameters	164	164	163	172	183
H-atom treatment	Constrained to parent site	Constrained to parent site	Constrained to parent site	Constrained to parent site	Constrained to parent site
Weighting scheme	$w = 1/[\sigma^2(F_o^2) + (0.0702P)^2 + 1.151P]$, where $P = (F_o^2 + 2F_c^2)/3$	$w = 1/[\sigma^2(F_o^2) + (0.0435P)^2 + 1.3394P]$, where $P = (F_o^2 + 2F_c^2)/3$	$w = 1/[\sigma^2(F_o^2) + (0.0954P)^2 + 0.4665P]$, where $P = (F_o^2 + 2F_c^2)/3$	$w = 1/[\sigma^2(F_o^2) + (0.1298P)^2]$, where $P = (F_o^2 + 2F_c^2)/3$	$w = 1/[\sigma^2(F_o^2) + (0.0501P)^2 + 1.7622P]$, where $P = (F_o^2 + 2F_c^2)/3$
$(\Delta/\sigma)_{max}$	< 0.0001	< 0.0001	< 0.0001	< 0.0001	< 0.0001
$\Delta\rho_{max}$, $\Delta\rho_{min}$ (e Å^{-3})	0.27, −0.43	0.29, −0.34	0.42, −0.47	0.33, −0.36	0.26, −0.29

	(VI)	(VII)	(VIII)	(IX)
Crystal data				
Chemical formula	$2C_{13}H_{14}N_6\cdot H_2O$	$2C_{13}H_{14}N_6O\cdot H_2O$	$C_{18}H_{16}N_6\cdot H_2O$	$2C_9H_{12}N_6\cdot C_2H_6O\cdot H_2O$
M_r	526.62	558.62	334.38	472.58
Cell setting, space group	Monoclinic, $C2/c$	Triclinic, $P\bar{1}$	Monoclinic, $P2_1/n$	Triclinic, $P\bar{1}$
Temperature (K)	120 (2)	120 (2)	120 (2)	120 (2)
a, b, c (Å)	17.642 (3), 18.278 (3), 8.3034 (18)	8.9516 (5), 12.0627 (7), 12.9053 (7)	10.1880 (11), 9.5136 (10), 33.695 (4)	7.9342 (15), 8.9219 (19), 16.767 (3)
α, β, γ (°)	90.00, 103.512 (17), 90.00	91.612 (4), 92.065 (3), 95.259 (5)	90.00, 93.131 (7), 90.00	76.855 (16), 83.505 (14), 88.003 (17)
V (Å^3)	2603.4 (9)	1386.06 (13)	3261.0 (6)	1148.3 (4)
Z	4	2	8	2
D_x (Mg m^{-3})	1.344	1.338	1.362	1.367
Radiation type	Mo $K\alpha$	Mo $K\alpha$	Mo $K\alpha$	Mo $K\alpha$
μ (mm^{-1})	0.09	0.09	0.09	0.10
Crystal form, colour	Plate, colourless	Block, colourless	Block, colourless	Plate, colourless
Crystal size (mm)	0.45 × 0.21 × 0.07	0.54 × 0.48 × 0.40	0.44 × 0.33 × 0.24	0.46 × 0.19 × 0.10
Data collection				
Diffractometer	Bruker–Nonius KappaCCD	Bruker–Nonius KappaCCD	Bruker–Nonius KappaCCD	Bruker–Nonius KappaCCD
Data collection method	φ and ω scans	φ and ω scans	φ and ω scans	φ and ω scans

Table 1 (continued)

	(VI)	(VII)	(VIII)	(IX)
Absorption correction	Multi-scan	Multi-scan	Multi-scan	Multi-scan
T_{min}	0.966	0.955	0.968	0.967
T_{max}	0.994	0.963	0.979	0.991
No. of measured, independent and observed reflections	32 439, 2987, 1829	31 433, 6316, 4620	83 278, 7493, 3887	28 718, 5275, 3372
Criterion for observed reflections	$I > 2\sigma(I)$	$I > 2\sigma(I)$	$I > 2\sigma(I)$	$I > 2\sigma(I)$
R_{int}	0.060	0.030	0.095	0.064
θ_{max} (°)	27.5	27.5	27.5	27.5
Refinement				
Refinement on	F^2	F^2	F^2	F^2
$R[F^2 > 2\sigma(F^2)]$, $wR(F^2)$, S	0.052, 0.159, 1.06	0.046, 0.104, 1.11	0.068, 0.220, 1.04	0.055, 0.163, 1.05
No. of reflections	2987	6316	7493	5275
No. of parameters	178	374	451	308
H-atom treatment	Constrained to parent site	Constrained to parent site	Constrained to parent site	Constrained to parent site
Weighting scheme	$w = 1/[\sigma^2(F_o^2) + (0.0797P)^2 + 1.7517P]$, where $P = (F_o^2 + 2F_c^2)/3$	$w = 1/[\sigma^2(F_o^2) + (0.025P)^2 + 1.067P]$, where $P = (F_o^2 + 2F_c^2)/3$	$w = 1/[\sigma^2(F_o^2) + (0.1085P)^2 + 1.9398P]$, where $P = (F_o^2 + 2F_c^2)/3$	$w = 1/[\sigma^2(F_o^2) + (0.0811P)^2 + 0.4703P]$, where $P = (F_o^2 + 2F_c^2)/3$
$(\Delta/\sigma)_{max}$	< 0.0001	0.001	< 0.0001	< 0.0001
$\Delta\rho_{max}$, $\Delta\rho_{min}$ (e Å^{-3})	0.27, −0.26	0.26, −0.28	0.42, −0.33	0.32, −0.32

Table 2
Selected torsional angles (°) in (I), (III) and (V)–(VIII).

	N*x*5—C*x*4—N*x*4—C*x*41	C*x*4—N*x*4—C*x*41—C*x*42
(I) x = nil	−178.66 (19)	−91.1 (3)
(III) x = nil	4.3 (5)	14.2 (5)
(V) x = nil	−170.51 (15)	68.7 (2)
(VI) x = nil	−175.65 (17)	78.2 (2)
(VII) x = 1	−174.76 (15)	76.1 (2)
(VII) x = 2	−175.73 (15)	78.1 (2)
(VIII) x = 1	−168.3 (2)	72.1 (4)
(VIII) x = 2	171.8 (2)	−68.3 (4)

imidines with hydrazine hydrate. Two procedures were employed for each: reaction in boiling ethanol (Boudet & Knochel, 2006; method A), and a solvent-free reaction under microwave irradiation (method B). In method A a mixture of the appropriate pyrimidine (0.02 mol) and hydrazine monohydrate (0.5 cm^3) in ethanol (5 cm^3) was heated under reflux for 0.5 h, and then cooled to ambient temperature. The resulting solid was collected by filtration, and washed successively with ethanol and diethyl ether to give the products (I)–(VIII). In method B mixtures of the pyrimidine and hydrazine monohydrate as used in method A were subjected to microwave irradiation (maximum power 300 W for 1 min at a controlled temperature of 373 K) using a CEM-Discover focused microwave reactor, in the absence of any additional solvent. The solid products were washed successively with ethanol and diethyl ether to give the products (I)–(VIII): the yields below refer to the products of method B. The high-resolution mass spectra were recorded in a Waters Micromass AutoSpec NT spectrometer. (I) yield 70%, m.p. 586–588 K, m/z 240.1122 ($C_{12}H_{12}N_6$ requires 240.1123); (II) yield 90%, m.p. 528–529 K, m/z 246.1576 ($C_{12}H_{18}N_6$ requires 246.1593); (III) yield 60%, m.p. 562–563 K, m/z 260.0565 ($C_{11}H_9{}^{35}ClN_6$ requires 260.0577); (IV) yield 60%, m.p. 523–524 K, m/z 263.1496 ($C_{11}H_{17}N_7O$ requires 263.1495); (V) yield 60%, m.p. 543–544 K, m/z 254.1286 ($C_{13}H_{14}N_6$ requires 254.1278); (VI) yield 70%, m.p. 548.5–549.3 K, 254.1272 ($C_{13}H_{14}N_6$ requires 254.1278); (VII) yield 73%, m.p. 478.5–479.5 K, m/z 270.1221 ($C_{13}H_{14}N_6O$ requires 270.1229); (VIII) yield 80%, m.p. 530–532 K, m/z 316.1430 ($C_{18}H_{16}N_6$ requires 316.1436); (IX) yield 50%, m.p. 560–561 K, m/z 204.1118 ($C_9H_{12}N_6$ requires 204.1123). Crystals suitable for single-crystal X-ray diffraction were grown by slow evaporation of solutions in conventional laboratory ethanol (ethanol/water, 97:3 v/v); these were colourless for (I)–(VIII) and yellow for (IX). The X-ray analyses showed that the crystals of (I)–(IV) were solvent free, those of (V) and (VIII) were stoichiometric monohydrates, those of (VI) and (VII) were stoichiometric hemihydrates, and those of (IX) were a hemihydrate ethanol hemisolvate. Also prepared by methods A and B was N^4-diethyl-1*H*-pyrazolo[3,4-d]pyrimidine-4,6-diamine (X): yield by method B 40%, m.p. 532–533 K, m/z 206.1278 ($C_9H_{14}N_6$ requires 206.1280), but the structure appears to be intractably disordered.

2.2. Data collection, structure solution and refinement

Details of cell data, data collection and structure solution and refinement are summarized in Table 1 (Burla *et al.*, 2005; Duisenburg *et al.*, 2000, 2003; Ferguson, 1999; Hooft, 1999; McArdle, 2003; Sheldrick, 2003, 2008; Spek, 2003). Unique assignments of space groups were made from the systematic absences for each of compounds (I)–(V) and (VIII). For (VI) the systematic absences permitted *C*2/*c* and *Cc* as possible space groups: *C*2/*c* was selected, and subsequently confirmed by structure analysis. Crystals of (VII) and (IX) are triclinic and for each the space group $P\bar{1}$ was selected, and subsequently confirmed by structure analysis. In cases where the asymmetric unit contained more than one pyrazolopyrimidine molecule, searches for possible addition symmetry using the ADDSYM option in *PLATON* (Spek, 2003) revealed none.

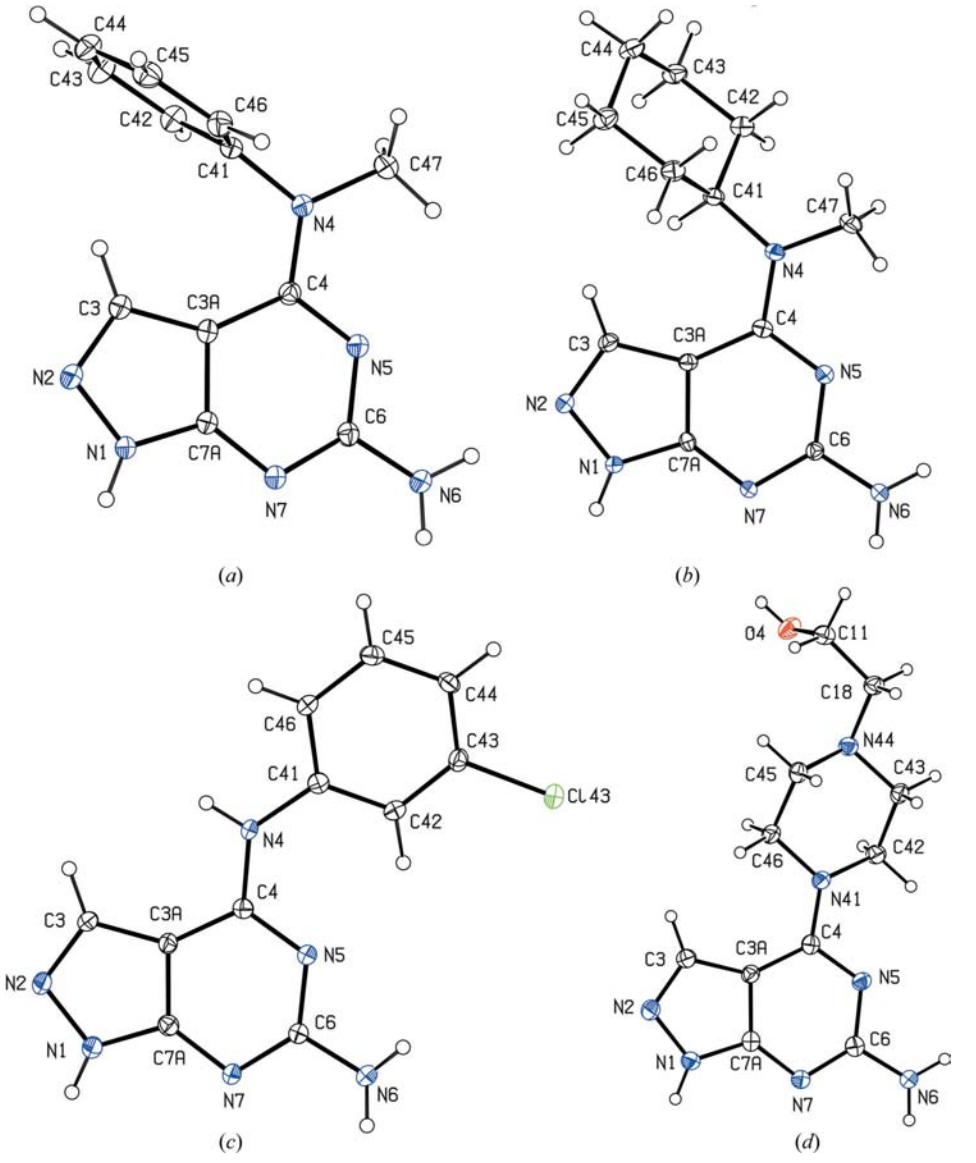

Figure 1
The molecular structures of the unsolvated compounds (I)–(IV), showing the atom-labelling schemes: (*a*) (I); (*b*) (II); (*c*) (III); (*d*) (IV). Displacement ellipsoids are drawn at the 30% probability level.

The structures were all solved by direct methods using *SHELXS*97 (Sheldrick, 2008), and refined on F^2 with all data using *SHELXL*97 (Sheldrick, 2008). A weighting scheme based upon $P = [F_o^2 + 2F_c^2]/3$ was employed in order to reduce statistical bias (Wilson, 1976).

All H atoms were located in difference maps: apart from the H atoms of the water molecules the H atoms were treated as riding atoms in geometrically idealized positions and with C—H distances of 0.95 (aromatic and heterocyclic), 0.98 (CH_3), 0.99 (CH_2) or 1.00 Å (aliphatic CH), N—H 0.86 Å and O—H 0.82 Å, with U_{iso}(H) = kU_{eq}(carrier), where k = 1.5 for the methyl and hydroxyl groups, and k = 1.2 for the other H atoms. For the H atoms in the water molecules, the O—H distances were restrained to 0.82 Å using *DFIX* restraints and these atoms were treated as riding atoms in the final cycles, with U_{iso}(H) = 1.5U_{eq}(O). Supramolecular analyses were made, and the diagrams were prepared with the aid of *PLATON* (Spek, 2003). Figs. 1 and 2 show the independent components and conformations of (I)–(IX) with the atom-labelling schemes, and Figs. 3–10 show aspects of the supramolecular structures. Selected torsional angles are given in Table 2 and details of the hydrogen bonding are in Table 3.[1]

3. Results and discussion

3.1. Crystallization behaviour

The crystals of (I)–(IX) used in this study were all grown from the same solvent, undried laboratory ethanol (*i.e.* ethanol/water, ~97:3 v/v), under the same conditions, slow evaporation while exposed to the normal laboratory atmosphere. Despite this consistency of crystallization procedure, (I)–(IV) crystallized in solvent-free form (Fig. 1) while (V)–(IX) all crystallized as solvates (Fig. 2). In these solvates (V)–(VIII) have all captured stoichiometric quantities of water from the solvent, while (IX) has crystallized with both ethanol and water present in stoichiometric quantities. Of the simple hydrates, (V) is a stoichiometric monohydrate, while (VI) and (VII) are both stoichiometric hemihydrates. As discussed in detail below (see §3.3.2), the patterns of the hydrogen bonding in the supramolecular structures formed by the pyrazolopyrimidine and water components in (VI)–(VII) and (IX) turn out to be almost identical. This is so, despite the different space groups for (VI), where the water component lies across a twofold rotation axis in the space group $C2/c$, and in (VII) where the water molecule lies in a general position in the space group $P\bar{1}$; it is so, despite the fact that (IX) is an ethanol hemisolvate as well as a hemihydrate. Since the ethanol component in (IX) is simply pendent from the hydrogen-bonded supramolecular

[1] Supplementary data for this paper are available from the IUCr electronic archives (Reference: BM5056). Services for accessing these data are described at the back of the journal.

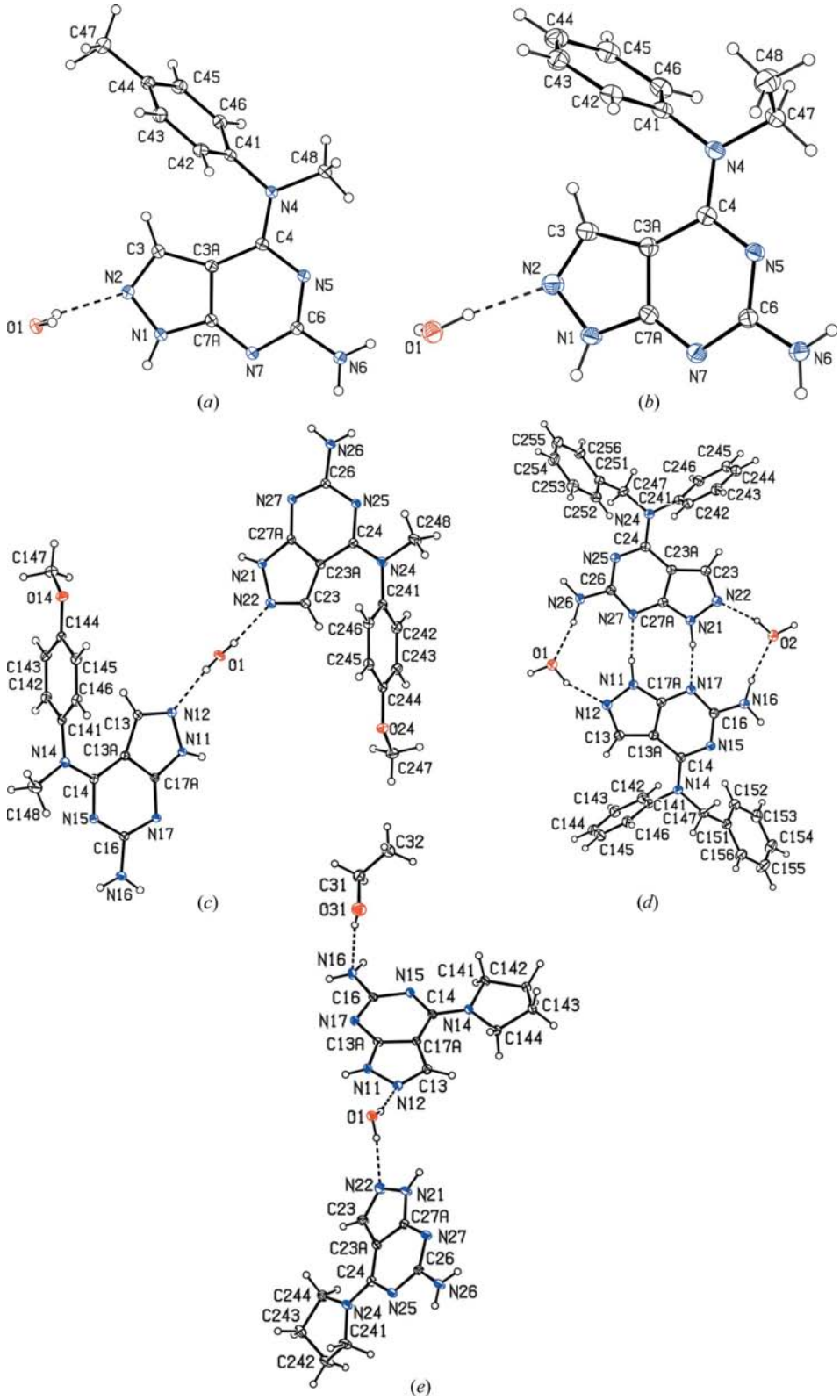

Figure 2
The independent molecular components in the solvated compounds (V)–(IX), showing the atom-labelling schemes and the O—H···N hydrogen bonds within the selected asymmetric units: (*a*) (V); (*b*) (VI), where the atom O1 lies on a twofold rotation axis; (*c*) (VII); (*d*) (VIII); (*e*) (IX). Displacement ellipsoids are drawn at the 30% probability level.

structure formed by the other components, it may reasonably be concluded that the structural role of the ethanol component in (VIII) is largely confined to the occupation of an otherwise void volume.

3.2. Molecular conformations

The cyclohexyl ring in (II) and the piperazine ring in (IV) both adopt chair conformations with the non-H substituents occupying equatorial sites. The two independent pyrrolidine rings in (VIII) have very similar values for the ring-puckering parameters (Cremer & Pople, 1975) φ_2, 272.1 (4) and 264.7 (4)° for the atom sequences (N*x*4, C*x*41, C*x*42, C*x*43, C*x*44) for x = 1 and 2, respectively, indicative of half-chair conformations where the rings are twisted about the lines joining the N*x*4 atoms to the mid-points of the bonds C*x*42—C*x*43.

For the compounds containing aryl substituents at the 4-amino position, the coordination at these N atoms is always planar within experimental uncertainty, so that the conformations of the organic components in these compounds can be defined in terms of just two torsional angles (Table 2). These data show firstly that the two independent pyrazolopyrimidine molecules in (VII) have almost identical conformations; secondly, that the N—C bonds of the substituted amino group are almost coplanar with the heterocyclic rings; thirdly, that in (I) and (V)–(VIII) the aryl ring is adjacent to the pyrazole ring, but in (III) the position of the aryl ring is remote from the pyrazole ring; and lastly, that the aryl ring is almost coplanar with the pyrazolopyrimidine ring in (III), but these ring systems are almost orthogonal in (I) and (V)–(VIII). The

Table 3
Hydrogen-bond parameters (Å, °).

D—H···A	D—H	H···A	D···A	D—H···A
(I)				
N1—H1···N7^{i}	0.86	1.99	2.841 (2)	172
N6—H6A···N2^{ii}	0.86	2.13	2.982 (3)	168
N6—H6B···N^{iii}	0.86	2.43	3.164 (3)	144
C3—H3···Cg1†	0.95	2.48	3.255 (3)	138
(II)				
N1—H1···N7^{i}	0.86	2.01	2.857 (3)	170
N6—H6A···N2^{ii}	0.86	2.13	2.959 (3)	161
N6—H6B···N5^{iii}	0.86	2.65	3.289 (3)	132
(III)				
N1—H1···N7^{iv}	0.86	2.06	2.901 (4)	167
N4—H4···N2^{v}	0.86	2.16	3.017 (3)	171
N6—H6B···Cl43^{vi}	0.86	2.75	3.504 (3)	148
C42—H42···N5	0.95	2.26	2.855 (4)	120
(IV)				
N1—H1···O4^{vii}	0.86	2.14	2.863 (4)	142
N1—H1···N44^{vii}	0.86	2.55	3.297 (4)	145
N6—H6A···N7^{viii}	0.86	2.26	3.074 (4)	157
N6—H6B···N5^{ix}	0.86	2.14	2.990 (4)	170
O4—H4···N2^{x}	0.82	1.99	2.796 (4)	167
(V)				
O1—H1A···N2	0.82	2.09	2.871 (2)	158
O1—H1B···N5^{xi}	0.82	2.05	2.858 (2)	168
N1—H1···O1^{iv}	0.86	2.00	2.857 (2)	176
N6—H6A···N7^{xii}	0.86	2.31	3.092 (2)	150
N6—H6B···O1^{xiii}	0.86	2.14	2.960 (2)	160
C3—H3···Cg1†	0.95	2.77	3.526 (2)	137
(VI)				
O1—H1A···N2	0.82	1.92	2.726 (2)	169
N1—H1···N7^{xiv}	0.86	2.11	2.971 (2)	179
N6—H6A···N5^{xv}	0.86	2.44	3.293 (3)	169
N6—H6B···O1^{xiv}	0.86	2.04	2.897 (2)	179
C3—H3···Cg1†	0.95	2.47	3.260 (3)	140
(VII)				
O1—H1A···N12	0.82	2.05	2.860 (2)	168
O1—H1B···N22	0.82	2.05	2.856 (2)	168
N11—H11···N17^{xvi}	0.86	2.01	2.868 (2)	174
N21—H21···N27^{xvii}	0.86	2.02	2.875 (2)	175
N16—H16A···N25^{xviii}	0.86	2.25	3.099 (2)	167
N26—H26A···N15^{xix}	0.86	2.23	3.076 (2)	170
N16—H16B···O1^{xvi}	0.86	2.21	3.059 (2)	169
N26—H26B···O1^{xvii}	0.86	2.22	3.073 (2)	170
C13—H13···Cg2‡	0.95	2.52	3.300 (2)	139
C23—H23···Cg3§	0.95	2.62	3.393 (2)	139
(VIII)				
O1—H1A···N12	0.98	1.89	2.813 (3)	155
O2—H2A···N22	0.98	1.83	2.774 (3)	160
O1—H1B···N15^{xx}	0.98	2.46	3.114 (3)	124
O2—H2B···N25^{xxi}	0.98	2.54	3.160 (3)	121
N11—H11···N27	0.98	1.90	2.872 (3)	172
N16—H16A···O2	0.98	2.12	3.045 (3)	156
N16—H16B···O1^{xxi}	0.98	2.11	2.988 (3)	148
N21—H21···N17	0.98	1.85	2.828 (3)	172
N26—H26A···O1	0.98	2.00	2.941 (3)	161
N26—H26B···O2^{xx}	0.98	2.08	2.997 (3)	156
C13—H13···Cg2‡	0.95	2.74	3.472 (3)	134
C23—H23···Cg3§	0.95	2.78	3.526 (3)	136
C244—H244···Cg4^{xxii}¶	0.95	2.65	3.563 (3)	161
(IX)				
O1—H1A···N12	0.82	1.97	2.773 (2)	164
O1—H1B···N22	0.82	1.96	2.767 (2)	169
N11—H11···N17^{i}	0.86	2.06	2.918 (2)	172
N21—H21···N27^{xxiii}	0.86	2.03	2.886 (2)	170
N16—H16A···N25^{xxiv}	0.86	2.24	3.088 (2)	169
N26—H26A···N15^{xxv}	0.86	2.32	3.172 (3)	171
N16—H16B···O1^{i}	0.86	2.14	2.988 (2)	168
N26—H26B···O1^{xxiii}	0.86	2.18	3.026 (2)	168
O31—H31···N16	0.82	2.21	3.021 (2)	168
C13—H13···O31^{xi}	0.95	2.47	3.371 (3)	159

Symmetry codes: (i) $1-x,-y,1-z$; (ii) $-\frac{1}{2}+x,\frac{1}{2}-y,-\frac{1}{2}+z$; (iii) $\frac{1}{2}-x,-\frac{1}{2}+y,\frac{1}{2}-z$; (iv) $1-x,2-y,1-z$; (v) $1-x,-\frac{1}{2}+y,\frac{1}{2}-z$; (vi) $x,1+y,z$; (vii) $\frac{3}{2}-x,-\frac{1}{2}-y,z$; (viii) $-\frac{1}{2}+x,\frac{1}{2}-y,1-z$; (ix) $\frac{1}{2}+x,\frac{1}{2}-y,1-z$; (x) $1-x,\frac{1}{2}+y,\frac{1}{2}-z$; (xi) $1-x,1-y,1-z$; (xii) $\frac{1}{2}-x,-\frac{1}{2}+y,z$; (xiii) $-\frac{1}{2}+x,\frac{3}{2}-y,1-z$; (xiv) $\frac{1}{2}-x,\frac{1}{2}-y,-z$; (xv) $-x,y,\frac{1}{2}-z$; (xvi) $-x,-y,1-z$; (xvii) $1-x,1-y,2-z$; (xviii) $x,-1+y,-1+z$; (xix) $x,1+y,1+z$; (xx) $-1+x,y,z$; (xxi) $1+x,y,z$; (xxii) $-\frac{1}{2}+x,\frac{1}{2}-y,-\frac{1}{2}+z$; (xxiii) $2-x,1-y,-z$; (xxiv) $-1+x,y,1+z$; (xxv) $1+x,y,-1+z$. † Cg1 is the centroid of ring (C41–C46). ‡ Cg2 is the centroid of ring (C141–C146). § Cg3 is the centroid of ring (C241–C246). ¶ Cg4 is the centroid of ring (C151–C156).

dihedral angles between the aryl and pyrazole rings are 87.0 (2), 78.0 (2) and 84.1 (2)° in (I), (V) and (VI), 84.47 (9) and 84.65 (9)° in the two independent molecules of (VII), and 79.7 (2) and 75.8 (2)° for the two independent molecules in (VIII), but only 14.4 (2)° in (III).

Closely associated with the conformations of (I) and (V)–(VIII) is a fairly short intermolecular C—H···π(arene) hydrogen bond in each molecule, in which the pyrazole C—H bond acts as the donor (Table 3); such an interaction is absent from the structure of (III). However, in (III), in contrast to (I) and (V)–(VIII), there is only a single hydrocarbyl substituent at the N4 atom leaving an N—H bond available for the formation of intermolecular hydrogen bonds and, in fact, this N—H bond participates in an almost linear intermolecular N—H···N interaction (see §3.3.1 and Table 3). Accordingly it is probable that the presence of this interaction controls the conformation about the C4—N4 bond in (III) (Table 2). For all of the N^4-aryl substituted examples here, (I), (III) and (V)–(VIII), two factors appear to be important in controlling the

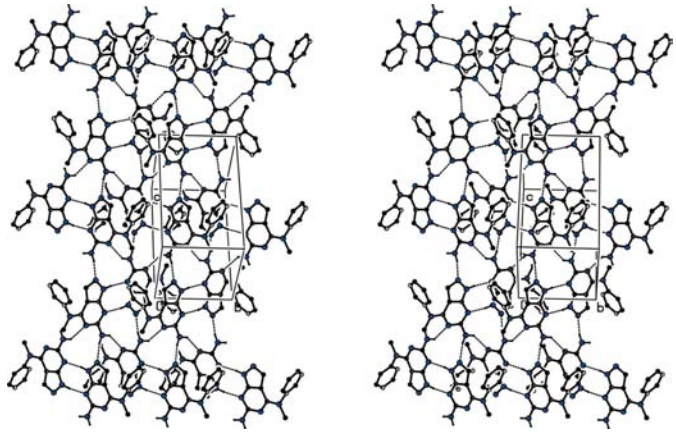

Figure 3
A stereoview of part of the crystal structure of (I), showing the formation of a hydrogen-bonded sheet parallel to (10$\bar{1}$). For the sake of clarity the H atoms bonded to C atoms have been omitted.

orientation of the N^4-aryl ring relative to the fused heterocyclic system. In (I) and (V)–(VIII) this aryl ring cannot approach coplanarity with the heterocyclic ring because of the resulting close and repulsive contacts between the H atom bonded to the pyrazole C atom and the H atoms of the aryl ring, whereas the formation of the C—H···π(arene) hydrogen bond to the non-coplanar ring is favourable. In (III) (Fig. 1*c*), on the other hand, there are no close intramolecular H···H contacts to preclude the near planarity of the whole molecular skeleton and, indeed, such planarity may be encouraged by the intramolecular C—H···N hydrogen bond (Table 3).

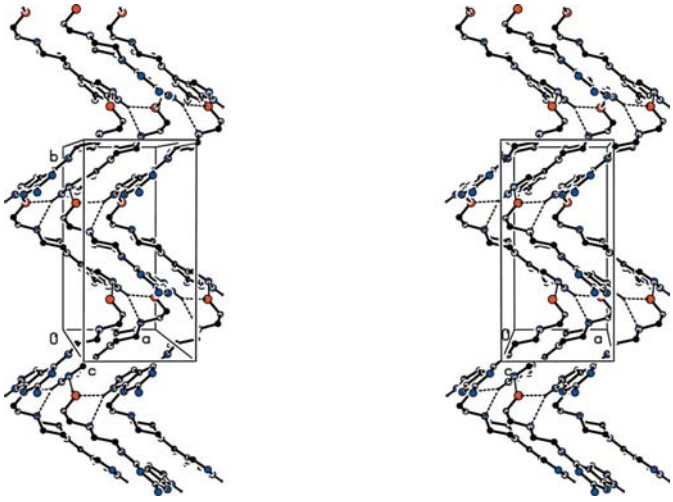

Figure 4
A stereoview of part of the crystal structure of (IV), showing the formation of a hydrogen-bonded sheet parallel to (001). For the sake of clarity the H atoms bonded to C atoms have been omitted.

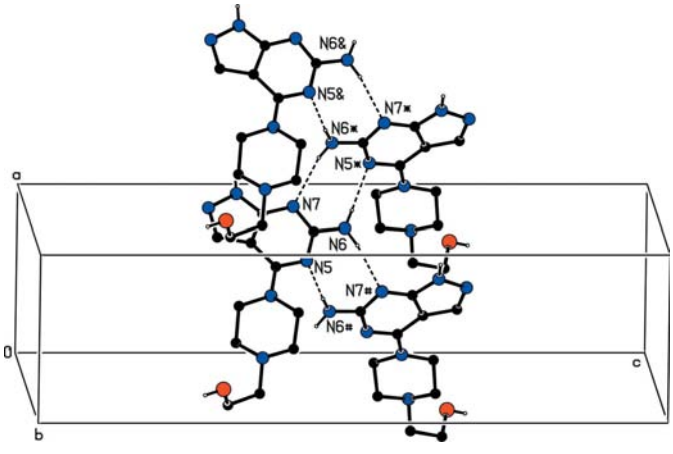

Figure 5
Part of the crystal structure of (IV) showing the formation of a chain of edge-fused $R_2^2(8)$ rings parallel to [100]. For the sake of clarity the H atoms bonded to C atoms have been omitted. The atoms marked with an asterisk (*), a hash (#) and an ampersand (&) are at the symmetry positions $(-\frac{1}{2}+x, \frac{1}{2}-y, 1-z)$, $(-\frac{1}{2}+x, \frac{1}{2}-y, 1-z)$ and $(1+x, y, z)$, respectively.

3.3. Crystal structures

The direction-specific interactions which are apparent within this series include hydrogen bonds of N—H···O, N—H···N, O—H···N, C—H···N, C—H···O and C—H···π(arene) types. Cogent criticism of the progressive relaxation of the definition of, and criteria for, significant hydrogen bonds (Cotton *et al.*, 1997) makes it desirable to specify the acceptance criteria for the hydrogen bonds considered in this study (Table 3). Of the interactions labelled as 'potential hydrogen bonds' by *PLATON* (Spek, 2003), we have discounted the following such interactions:

(i) all C—H···N contacts in which the H···N distance exceeds 2.60 Å, and

(ii) all C—H···N contacts in which the C—H bond is part of a methyl group.

It has been shown by solid-state NMR spectroscopy (Riddell & Rogerson, 1996, 1997) that hydrocarbyl substituents including methyl groups CH_3—E (where E represents the atom to which the methyl group is bonded) generally undergo very rapid rotation about the C—E bond even at low temperatures in the solid state, so that the apparent H-atom sites in effect represent not static positions, but merely the energy minima of the rotational potential-energy function; these contacts in the present series are, in fact, nearly all intramolecular with apparent C—H···N angles less than 105°. The intermolecular C—H···Cl contact in (III) is discussed below (see §3.3.1).

3.3.1. Unsolvated structures. Compounds (I) and (II): Although (I) and (II) are by no means isomorphous, nor even isostructural, judging from the atomic coordinates, nonetheless, the actions of the intermolecular hydrogen bonds and the resulting supramolecular structures are very similar. We discuss the supramolecular structure of (I) in detail and then draw brief comparisons between (I) and (II).

Three N—H···N hydrogen bonds, one of them rather weak (Table 3), link the molecules of (I) into sheets generated by the combination of an inversion operation and a glide plane. The stronger two of the hydrogen bonds suffice to form the sheet, and this is modestly reinforced by the third, weaker interaction. The pyrazole ring N1 atom in the molecule at

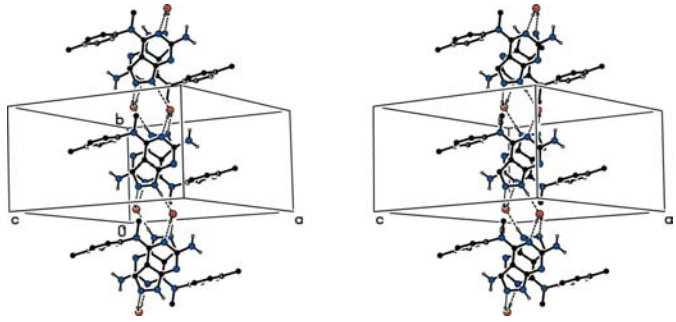

Figure 6
A stereoview of part of the crystal structure of (V), showing the formation of a hydrogen-bonded chain of $R_4^4(10)$ and $R_4^4(16)$ rings parallel to [010]. For the sake of clarity the H atoms bonded to C atoms have been omitted.

(x, y, z) acts as a hydrogen-bond donor to the pyrimidine ring N7 atom in the molecule at $(1-x, -y, 1-z)$, so forming a centrosymmetric $R_2^2(8)$ dimer (Bernstein *et al.*, 1995), centred at $(\frac{1}{2}, 0, \frac{1}{2})$. The formation of this $R_2^2(8)$ motif built from a pair of N—H···N hydrogen bonds is, in fact, common to most of the structures reported here except for those of (IV) and (V), in each of which the N1—H1 bond forms a hydrogen bond of the type N—H···O. This cyclic motif is centrosymmetric in each of (I)–(III) and (VI); in (VII) and (IX), where $Z' = 2$, each independent type of molecule forms a centrosymmetric motif of this type; and in (VIII), which also crystallizes with $Z' = 2$, the two independent pyrimidine components form a similar motif which is approximately, although not crystallographically centrosymmetric.

In addition, the amino atom N6 in the molecule at (x, y, z) acts as a hydrogen-bond donor to the pyrazole ring N2 atom in the molecule at $(-\frac{1}{2}+x, \frac{1}{2}-y, -\frac{1}{2}+z)$, which itself forms part of the $R_2^2(8)$ dimer centred at $(0, \frac{1}{2}, 0)$. This hydrogen bond thus links the dimer centred at $(\frac{1}{2}, 0, \frac{1}{2})$ to the four dimers centred at $(0, \frac{1}{2}, 0)$, $(0, -\frac{1}{2}, 0)$, $(1, \frac{1}{2}, 1)$ and $(1, -\frac{1}{2}, 1)$, thereby generating a sheet parallel to $(10\bar{1})$ (Fig. 3). The weak hydrogen bond reinforces this sheet, but does not link it to the neighbouring sheet: there are, in fact, no direction-specific intermolecular interactions between adjacent sheets. In (II) the intermolecular contact having N5 as the acceptor has much longer H···N and N···N distances than the corresponding contact in (I) (Table 3), and in (II) this contact cannot be regarded as structurally significant. Nonetheless, the actions of the other two N—H···N hydrogen bonds are identical in (II) to those in (I), forming a sheet parallel to $(10\bar{1})$.

Compound (III): Compound (III) differs significantly from (I) and (II), not only in its overall conformation (see §3.2), but in containing an additional amino N—H bond which thus increases the number of potential hydrogen-bond donors. However, the supramolecular aggregation, like that in (I) and (II), is two-dimensional and the formation of the sheet structure generated by the combination of an inversion operation and a 2_1 screw axis depends upon just two N—H···N hydrogen bonds, with N1 and N4 atoms as the donors. As in (I) and (II), atoms N1 and N7 are utilized in the formation of a cyclic $R_2^2(8)$ dimer, this time centred at $(\frac{1}{2}, 1, \frac{1}{2})$: the second N—H···N hydrogen bond, with N4 as the donor, then links the dimer centred at $(\frac{1}{2}, 1, \frac{1}{2})$ to the four dimers centred at $(\frac{1}{2}, \frac{1}{2}, 0)$, $(\frac{1}{2}, \frac{1}{2}, 1)$, $(\frac{1}{2}, \frac{3}{2}, 0)$ and $(\frac{1}{2}, \frac{3}{2}, 1)$, so forming a sheet parallel to (100). The role of the $-NH_2$ group in the supramolecular aggregation in (III) is extremely modest. For the N6—H6*A* bond there is no potential hydrogen-bond acceptor of any kind close enough to form any significant interaction, while the N6—H6*B* bond in the molecule at (x, y, z) forms a fairly long contact with the Cl atom of the molecule at $(x, 1+y, z)$. Hydrogen bonds of the type N—H···Cl—C are comparatively uncommon (Aullón *et al.*, 1998), and recent interpretations of such contacts place them right at the outer limit of hydrogen bonding, where this gives way to simple van der Waals contacts (Brammer *et al.*, 2001; Thallypally & Nangia, 2001). The contact of this type in (III) lies within the sheet generated by the N—H···N hydrogen bonds and thus, whatever its significance as a hydrogen bond, it can have no effect on the overall dimensionality of the supramolecular aggregation.

Compound (IV): The molecules of (IV) are linked into a three-dimensional framework structure by a combination of one three-centre N—H···(O,N) hydrogen bond, two independent N—H···N hydrogen bonds and one O—H···N hydrogen bond (Table 3). The formation of the framework is readily analysed in terms of three one-dimensional substructures.

The pyrazole ring N1 atom in the molecule at (x, y, z) acts as a hydrogen-bond donor to the O4 and N44 atoms, both in

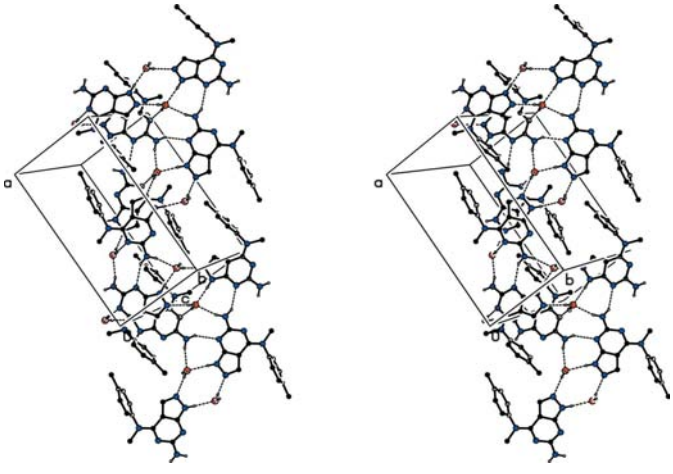

Figure 7
A stereoview of part of the crystal structure of (V), showing the formation of a hydrogen-bonded sheet parallel to (001). For the sake of clarity the H atoms bonded to C atoms have been omitted.

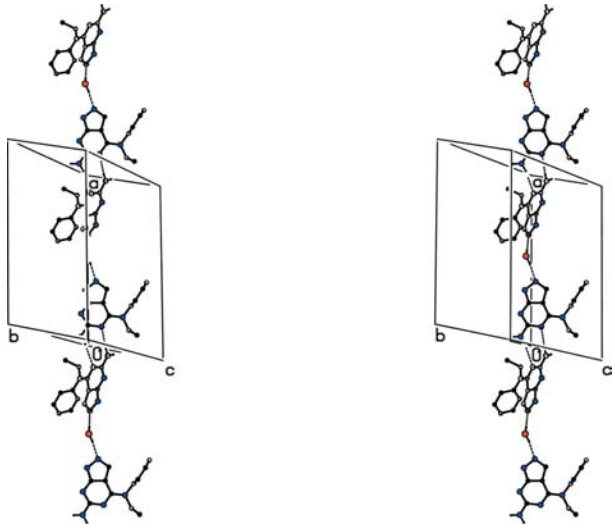

Figure 8
A stereoview of part of the crystal structure of (VI), showing the formation of a hydrogen-bonded chain of rings parallel to [100]. For the sake of clarity the H atoms bonded to C atoms have been omitted.

the molecule at $(\frac{3}{2}-x,\ -\frac{1}{2}+y, z)$ in an asymmetric three-centre interaction, forming a $C(9)C(12)[R_1^2(5)]$ chain of rings running parallel to the [010] direction and generated by the *b* glide plane at $x = 0.75$. In addition, the hydroxyl O4 atom in the molecule at (x, y, z) acts as a hydrogen-bond donor to the pyrimidine ring N2 atom in the molecule at $(1-x, \frac{1}{2}+y, \frac{1}{2}-z)$, so forming a second chain running parallel to the [010] direction, this time of the type $C(10)$ generated by the 2_1 screw axis along $(\frac{1}{2}, y, \frac{1}{4})$. The combination of these two chains parallel to [010] generates a rather complex sheet parallel to (001) (Fig. 4). Two sheets of this type, generated by the screw axes at $y = 0.25$ and $y = 0.75$, respectively, pass through each unit cell and adjacent sheets are linked by a third one-dimensional substructure. In this third substructure, the amino atom N6 in the molecule at (x, y, z) acts as a hydrogen-bond donor, *via* H6*A* and H6*B*, respectively, to the pyrimidine ring atoms N7 and N5 in the molecules at $(-\frac{1}{2}+x, \frac{1}{2}-y, 1-z)$ and $(\frac{1}{2}+x, \frac{1}{2}-y, 1-z)$, respectively. These two hydrogen bonds thus form a chain of edge-fused rings containing two independent $R_2^2(8)$ motifs, running parallel to the [100] direction and generated by the 2_1 screw axis along $(x, \frac{1}{4}, \frac{1}{2})$ (Fig. 5). Since the molecule at (x, y, z) and the two at $(\pm\frac{1}{2}+x, \frac{1}{2}-y, 1-z)$ lie in different sheets, the effect of this chain of rings motif is to link the (001) sheets into a three-dimensional framework structure.

3.3.2. Hydrated structures. Compound (V): This compound is a stoichiometric monohydrate and the asymmetric unit was selected such that the two molecular components within it are linked by an O—H···N hydrogen bond (Table 3): this two-component aggregate can then be regarded as the basic building block within the structure. There are then one O—H bond and three N—H bonds available to provide the donors in hydrogen bonds external to the two-component building block; despite this large number of donors, the hydrogen-bonded supramolecular structure is only two-dimensional. The formation of the sheet structure of (V) is most easily analysed in terms of a single one-dimensional substructure.

The water atom O1 and the pyrazole ring atom N1 in the aggregate at (x, y, z) act as hydrogen-bond donors to the ring atom N5 at $(1-x, 1-y, 1-z)$ and the water atom O1 at $(1-x, 2-y, 1-z)$. The propagation by inversion of these two hydrogen bonds generates a chain of edge-fused centrosymmetric rings running along $(\frac{1}{2}, y, \frac{1}{2})$, with $R_4^4(10)$ rings centred at $(\frac{1}{2}, n, \frac{1}{2})$ (where *n* represents zero or an integer) alternating with $R_4^4(16)$ rings centred at $(\frac{1}{2}, n+\frac{1}{2}, \frac{1}{2})$ (where *n* represents zero or an integer; Fig. 6).

Two further hydrogen bonds link chains of this type into a sheet. The amino N6 atom at (x, y, z) acts as a hydrogen-bond donor, *via* H6*A* and H6*B*, respectively, to the atom O1 at $(-\frac{1}{2}+x, \frac{3}{2}-y, 1-z)$ and N7 at $(\frac{1}{2}-x, -\frac{1}{2}+y, z)$. The latter two aggregates are, in fact, components of the chain of edge-fused rings running along $(0, y, \frac{1}{2})$, and propagation by inversion of the two hydrogen bonds links successive chains running along $(\frac{1}{2}, y, \frac{1}{2})$ into a sheet parallel to (001) (Fig. 7).

Compounds (VI) and (VII): The organic component in (VI) is isomeric with that in (V): however, (VI) crystallizes as a stoichiometric hemihydrate, as opposed to the monohydrate (V), in which the water molecule lies across a twofold rotation axis in the space group *C*2/*c*. The asymmetric unit was selected such that the two independent components are linked by an O—H···N hydrogen bond, just as for (V), with the water O atom lying on the axis along $(\frac{1}{2}, y, \frac{1}{4})$. The basic building block in the supramolecular structure can thus be taken as a three-component aggregate, lying across a twofold rotation axis and consisting of one water molecule and two pyrazolopyrimidine molecules. Hence there are six N—H bonds per aggregate available for the formation of hydrogen bonds external to the aggregate. As with (V), the hydrogen-bonded structure is only two-dimensional and its formation is best analysed in terms of two one-dimensional substructures, neither of which utilizes all of the available hydrogen bonds.

In the simpler of the two substructures, the amino N6 atoms in the organic molecules at (x, y, z) and $(1-x, y, \frac{1}{2}+z)$, which form parts of the reference aggregate lying across the rotation axis along $(\frac{1}{2}, y, \frac{1}{4})$, act as donors to the pyrimidine ring N5 atoms at $(-x, y, \frac{1}{2}-z)$ and $(1+x, y, z)$, respectively, which themselves form parts of the aggregates lying across the axes $(-\frac{1}{2}, y, \frac{1}{4})$ and $(\frac{3}{2}, y, \frac{1}{4})$, respectively. Hence, propagation of this

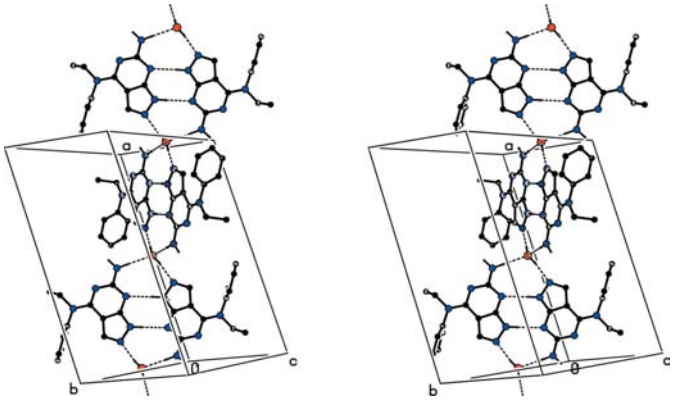

Figure 9
A stereoview of part of the crystal structure of (VI), showing the formation of a hydrogen-bonded chain of spiro-fused and edge-fused rings parallel to [101]. For the sake of clarity the H atoms bonded to C atoms have been omitted.

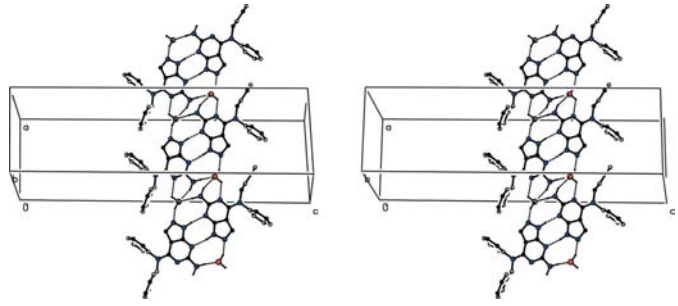

Figure 10
A stereoview of part of the crystal structure of (VIII), showing the formation of a hydrogen-bonded chain parallel to [100], which contains six independent types of ring. For the sake of clarity the H atoms bonded to C atoms have been omitted.

hydrogen bond by successive rotations generates a $C_3^3(15)C_3^3(15)[R_2^2(8)]$ chain of rings running parallel to the [100] direction (Fig. 8).

The second substructure is more complex and it is generated by a combination of rotations and inversions. The pyrazole ring N1 atom and the amino N6 atom, both at (x, y, z), act as hydrogen-bond donors, respectively, to the pyrimidine ring atom N7 and the water atom O1, both at $(\frac{1}{2} - x, \frac{1}{2} - y, -z)$. These interactions generate a centrosymmetric tricyclic motif, centred at $(\frac{1}{4}, \frac{1}{4}, 0)$, in which an $R_2^2(8)$ ring is concentric with an $R_4^4(18)$ ring (Fig. 9), which itself is partitioned by the smaller ring into one $R_2^2(8)$ portion and two symmetry-related $R_3^3(9)$ portions. The propagation of this motif by rotation and inversion then generates a complex chain of spiro-fused and edge-fused rings running parallel to the [101] direction (Fig. 9). The combination of the chains parallel to [100] and [101] generates a sheet parallel to (010), although there are no significant direction-specific interactions between adjacent sheets.

Compound (VII), like (VI), crystallizes as a stoichiometric hemihydrate but, unlike that in (VI), the asymmetric unit in (VII) contains two independent pyrazolopyrimidine components and one water molecule, all occupying general positions in the space group $P\bar{1}$. Within the selected asymmetric unit (Fig. 2*c*) the three components are linked by two independent O—H···N hydrogen bonds (Table 3). Despite the absence of any crystallographic symmetry within the three-component aggregate, this does nonetheless exhibit approximate local twofold rotational symmetry, of the type observed in (VI). The approximate symmetry is also manifested both in the pattern of the hydrogen bonds formed by the two independent organic components, and in the dimensions of these hydrogen bonds (Table 3).

As in (VI), there are six N—H bonds available for the formation of hydrogen bonds exterior to the basic three-component aggregate, but in (VII) they are all independent. These hydrogen bonds combine to generate a two-dimensional structure, which strongly mimics that in (VI), although with different orientations both for the overall sheet structure and for its two-component substructures, consequent upon the different crystal systems utilized by (VI) and (VII). In the simpler of the two substructures in (VII), the amino atoms N16 and N26 in the aggregate at (x, y, z) act as hydrogen-bond donors *via* H16*A* and H26*A*, respectively, to atoms N25 at $(x, -1 + y, -1 + z)$ and N15 at $(x, 1 + y, 1 + z)$, so generating by translation a chain of rings running parallel to the [011] direction. This chain has the same topology as the chain of rings in (VI), although this latter chain runs parallel to the [100] direction and it is generated by rotation rather than by translation.

The second one-dimensional substructure in (VII) also closely mimics the corresponding substructure in (VI). The ring N11 atom and the amino N16 atom at (x, y, z) act as hydrogen-bond donors, respectively, to the ring N17 atom and the water O1 atom, both at $(-x, -y, 1 - z)$, so generating by inversion concentric $R_2^2(8)$ and $R_4^4(18)$ rings centred at $(0, 0, \frac{1}{2})$: similarly, the N21 and N26 atoms at (x, y, z) acts as donors to the N27 and O1 atoms, both at $(1 - x, 1 - y, 2 - z)$ so generating a similar motif, this time centred at $(\frac{1}{2}, \frac{1}{2}, 1)$. The combination of these four hydrogen bonds, together with the two O—H···N hydrogen bonds within the asymmetric unit, then generates a chain of spiro-fused and edge-fused rings running parallel to the [111] direction with the same topology as the [101] chain in (VI). This differs from the comparable chain in (VI) firstly in its [111] direction in (VII) as opposed to [101] in (VI), and secondly in its mode of generation, which depends entirely on inversion as opposed to inversion and rotation in (VI), and finally in containing two independent concentric ring motifs, where (VI) contains just one of these motifs. In (VII) the chains parallel to [011] and [111] combine to form a sheet parallel to $(01\bar{1})$, whose construction closely mimics that of the (010) sheet in (VI). Thus, the overall supramolecular aggregation in (VI) and (VII) is very similar despite their different space groups, crystal systems and Z' values.

Compound (VIII): The asymmetric unit selected for (VIII) (Fig. 2*d*) exhibits approximate, although non-crystallographic centrosymmetry such that the four-component aggregate is centred at approximately (0.54, 0.33, 0.62): no additional crystallographic symmetry was detected. The approximate nature of this inversion relationship is illustrated both by the location of the centre of the aggregate and by the leading torsional angles (Table 2), where the corresponding angles in the two independent pyrimidine components have opposite signs, but with magnitudes whose differences are statistically significant.

The independent components within the selected asymmetric unit are linked by six hydrogen bonds, two each of O—H···N, N—H···N and N—H···O types (Table 3) in a form of multipoint recognition involving one $R_2^2(8)$ ring flanked by two similar but independent $R_3^3(9)$ rings (Fig. 2*d*). Hence there are only two O—H and two N—H bonds per aggregate available for the formation of hydrogen bonds between adjacent aggregates. Thus, two O—H···N and two N—H···O hydrogen bonds link the four-molecule aggregates into a complex chain of edge-fused rings running parallel to the [100] direction. The four-point linkages between the pseudo-centric aggregates involve one $R_4^2(8)$ ring and two similar but independent $R_2^2(6)$ rings, so that overall the chain contains six independent ring types (Fig. 10). A single C—H···π(arene) hydrogen bond links adjacent chains of rings into sheets: the aryl atom C244 at (x, y, z) acts as a donor to the ring (C151–C156) at $(-\frac{1}{2} + x, \frac{1}{2} - y, -\frac{1}{2} + z)$, thereby generating a chain running parallel to the [101] direction, whose action is to link the *d* chains of rings along [100] into a sheet parallel to (010).

Compound (IX): This compound crystallizes with one molecule of water and one molecule of ethanol per two molecules of pyrazolopyrimidine, and all of the independent molecular components lie in general positions in the space group $P\bar{1}$ (Fig. 2*e*). The asymmetric unit was selected so that the water molecule is linked to the organic components by two independent O—H···N hydrogen bonds (Table 3), exactly as in (VII). The ethanol is further linked to this three-component aggregate by a further O—H···N hydrogen bond; its only

other role in the supramolecular structure is to act as the acceptor in a C—H···O hydrogen bond which lies within the sheet structure generated by the other three components. Accordingly its presence does not appear materially to influence the overall supramolecular structure.

Apart from the pendent ethanol molecules, the formation of the sheet structure in (IX) closely mimics those in (VI) and (VII), in that the sheet itself and the two-component substructure have the same topology as those discussed earlier. In (IX), the simpler of the two substructures, that generated by translation, runs parallel to the $[10\bar{1}]$ direction, as opposed to [011] in (VII), while the more complex of the substructures in (IX), that generated by inversion, runs parallel to the $[11\bar{1}]$ direction, as against [111] in (VII). Hence the resulting sheet structure in (IX) lies parallel to (101) compared with the $(01\bar{1})$ sheet in (VII).

4. Concluding discussion

The number of types of direction-specific intermolecular interaction manifested in the structures discussed here is small. In the structure of the solvent-free compounds (I)–(III), all of the intermolecular interactions are N—H···N hydrogen bonds: in the structure of (IV) and in those of the solvates (V)–(IX) there are, in addition, intermolecular O—H···N and N—H···O hydrogen bonds. However, there are no intermolecular C—H···N hydrogen bonds, nor any aromatic $\pi\cdots\pi$ stacking interactions anywhere in this series; a C—H···O hydrogen bond occurs only in (IX), while an intermolecular C—H···π(arene) hydrogen bond occurs only in (VIII). Thus, in summary, where O—H bonds are present in this series, the intermolecular hydrogen bonds can be of O—H···N, N—H···N and N—H···O types, but where O—H bonds are absent, the intermolecular hydrogen bonds are mainly of the type N—H···N.

For the series (I)–(IX) we note the following general points.

(i) Intramolecular C—H···π(arene) interactions appear to have a significant influence on the molecular conformation of (I), and (V)–(VIII).

(ii) Centrosymmetric, or approximately centrosymmetric $R_2^2(8)$ motifs of paired N—H···N hydrogen bonds occur in all compounds apart from (IV) and (V).

(iii) Despite the different compositions and constitutions of (I)–(III), their supramolecular structures are topologically very similar with sheets formed by the combination of an inversion operation with either a glide plane, as in (I) and (II), or a 2_1 screw axis, as in (III).

(iv) In the hemihydrates (VI), (VII) and (IX) the hydrogen-bonding action of the water components are the same, with the O—H···N hydrogen bonds all having the two-coordinate N atoms of the pyrazole rings as acceptors.

(v) Possibly following from this, the supramolecular structures of (VI), (VII) and (IX) are very similar, despite the different space group and Z' value in (VI) and the presence of the ethanol component in (IX). The strong similarity between the hydrogen-bonded topology in (VI) and (VII), in particular where the Z' values are $\frac{1}{2}$ and 1, respectively, agrees well with the conclusion (Pidcock, 2006), based on the application of the Box Model of crystal packing (Pidcock & Motherwell, 2003) to structures retrieved from in the Cambridge Structural Database (Allen, 2002), that, statistically, the packing arrangements in organic structures with $Z' = 2$ are almost indistinguishable from those in structures having $Z' = 1$, at least in triclinic structures and those in the more common monoclinic and orthorhombic space groups.

(vi) Amongst the hydrates in this series space group No. 14 ($P2_1/c$ or $P2_1/n$) occurs only once, for (VIII) although this is the most common space group observed for hydrates in general (Cruz Cabeza *et al.*, 2007) and for unsolvated molecular structures as a whole, where the evolution of space-group frequencies has been summarized by Brock & Dunitz (1994), who noted that the dominance of organic structures by just a few space groups was already apparent over 50 years ago. However, for solvates as a whole, it is interesting to note that $P\bar{1}$ is the commonest space group, with a particularly high frequency observed for benzene and toluene solvates (Cruz Cabeza *et al.*, 2007).

The apparent simplicity found in the present series (I)–(IX), which may be sufficiently robust to be of predictive value, must be contrasted with the behaviour which we have previously observed in a number of other extended series of cognate structures (Glidewell *et al.*, 2002, 2004, 2005, 2006; Melguizo *et al.*, 2003; Quesada *et al.*, 2004; Cuffini *et al.*, 2006; Wardell *et al.*, 2006, 2007), where no one structure in any series could readily be predicted even from a detailed knowledge of each of the remaining structures in that series because, very commonly, no two structures in a given series manifested the same range of direction-specific intermolecular interactions. A significant source of unpredictability in the present series concerns the presence or absence of solvation in the crystal structure. It is by no means obvious why, for example, (V) crystallizes as a monohydrate, while (I) crystallizes in solvent-free form; or why (V) and (VI), where the organic components are isomeric, crystallize as a monohydrate and as a hemihydrate respectively; or why (V) and (VII), again with very similar constitutions for the organic components, crystallize respectively as a monohydrate and as a hemihydrate.

X-ray data were collected at Servicios Técnicos de Investigación, Universidad de Jaén, Spain. JC, AM and MN thank the Consejería de Innovación, Ciencia y Empresa (Junta de Andalucía, Spain) and the Universidad de Jaén for financial support. JT and JQ thank COLCIENCIAS and UNIVALLE (Universidad del Valle, Colombia) for financial support.

References

Allen, F. H. (2002). *Acta Cryst.* B**58**, 380–388.
Aullón, G., Bellamy, D., Brammer, L., Bruton, E. A. & Orpen, A. G. (1998). *Chem. Commun.* pp. 653–654.
Avasthi, K., Bal, C., Sharon, A. & Maulik, P. R. (2003). *Acta Cryst.* C**59**, o494–o495.
Avasthi, K., Bhagat, D., Bal, C., Sharon, A., Yadav, U. & Maulik, P. R. (2003). *Acta Cryst.* C**59**, o409–o412.

Avasthi, K., Farooq, S. M., Tewari, A. K., Sharon, A. & Maulik, P. R. (2003). *Acta Cryst.* C**59**, o42–o45.
Avasthi, K., Rawat, D. S., Chandra, T., Sharon, A. & Maulik, P. R. (2002). *Acta Cryst.* C**58**, o311–o313.
Avasthi, K., Rawat, D. S., Sarkhel, S. & Maulik, P. R. (2002). *Acta Cryst.* C**58**, o325–o327.
Avasthi, K., Tewari, A., Rawat, D. S., Sharon, A. & Maulik, P. R. (2002). *Acta Cryst.* C**58**, o494–o495.
Bernstein, J., Davis, R. E., Shimoni, L. & Chang, N.-L. (1995). *Angew. Chem. Int. Ed. Engl.* **34**, 1555–1573.
Biswas, G., Chandra, T., Garg, N., Bhakuni, D. S., Pramanik, A., Avasthi, K. & Maulik, P. R. (1996). *Acta Cryst.* C**52**, 2563–2566.
Boudet, N. & Knochel, P. (2006). *Org. Lett.* **8**, 3737–3740.
Brammer, L., Bruton, E. A. & Sherwood, P. (2001). *Cryst. Growth Des.* **1**, 277–290.
Brock, C. P. & Dunitz, J. D. (1994). *Chem. Mater.* **6**, 1118–1127.
Burla, M. C., Caliandro, R., Camalli, M., Carrozzini, B., Cascarano, G. L., De Caro, L., Giacovazzo, C., Polidori, G. & Spagna, R. (2005). *J. Appl. Cryst.* **38**, 381–388.
Cotton, F. A., Daniels, L. M., Jordan, G. T. & Murillo, C. A. (1997). *Chem. Commun.* pp. 1673–1674.
Cremer, D. & Pople, J. A. (1975). *J. Am. Chem. Soc.* **97**, 1354–1358.
Cruz Cabeza, A. J., Pidcock, E., Day, G. M., Motherwell, W. D. S. & Jones, W. (2007). *CrystEngComm*, **9**, 556–560.
Cuffini, S., Glidewell, C., Low, J. N., de Oliveira, A. G., de Souza, M. V. N., Vasconcelos, T. R. A., Wardell, S. M. S. V. & Wardell, J. L. (2006). *Acta Cryst.* B**62**, 651–665.
Duisenberg, A. J. M., Hooft, R. W. W., Schreurs, A. M. M. & Kroon, J. (2000). *J. Appl. Cryst.* **33**, 893–898.
Duisenberg, A. J. M., Kroon-Batenburg, L. M. J. & Schreurs, A. M. M. (2003). *J. Appl. Cryst.* **36**, 220–229.
Ferguson, G. (1999). *PRPKAPPA*. University of Guelph, Canada.
Glidewell, C., Howie, R. A., Low, J. N., Skakle, J. M. S., Wardell, S. M. S. V. & Wardell, J. L. (2002). *Acta Cryst.* B**58**, 864–876.
Glidewell, C., Low, J. N., Skakle, J. M. S. & Wardell, J. L. (2006). *Acta Cryst.* B**62**, 666–675.
Glidewell, C., Low, J. N., Skakle, J. M. S., Wardell, S. M. S. V. & Wardell, J. L. (2005). *Acta Cryst.* B**61**, 227–237.
Glidewell, C., Low, J. N., Skakle, J. M. S., Wardell, S. M. S. V. & Wardell, J. L. (2004). *Acta Cryst.* B**60**, 472–480.
He, J.-L., Seela, F., Eickmeier, H. & Reuter, H. (2002). *Acta Cryst.* C**58**, o593–o595.
Hooft, R. W. W. (1999). *COLLECT*. Nonius BV, Delft, The Netherlands.
Larson, S. B., Anderson, J. D., Revankar, G. R. & Robins, R. K. (1988). *Acta Cryst.* C**44**, 191–193.
Lin, W., Xu, K., Eickmeier, H. & Seela, F. (2005). *Acta Cryst.* C**61**, o195–o197.
Maulik, P. R., Avasthi, K., Sarkhel, S., Chandra, T., Rawat, D. S., Logsdon, B. & Jacobson, R. A. (2000). *Acta Cryst.* C**56**, 1361–1363.
McArdle, P. (2003). *OSCAIL for Windows*, Version 10. Crystallography Centre, Chemistry Department, NUI Galway, Ireland.
Melguizo, M., Quesada, A., Low, J. N. & Glidewell, C. (2003). *Acta Cryst.* B**59**, 263–276.
Moukha-Chafiq, O., Taha, M. L., Lazrek, H. B., Vasseur, J.-J. & De Clercq, E. (2006). *Nucleosides Nucleotides Nucleic Acids*, **25**, 849–860.
Novinson, T., Bhooshan, B., Okabe, T., Revankar, G. R., Robins, R. K., Senga, K. & Wilson, H. R. (1976). *J. Med. Chem.* **19**, 512–516.
Pidcock, E. (2006). *Acta Cryst.* B**62**, 268–279.
Pidcock, E. & Motherwell, W. D. S. (2003). *Chem. Commun.* pp. 3028–3029.
Portilla, J., Quiroga, J., Cobo, J., Low, J. N. & Glidewell, C. (2005). *Acta Cryst.* C**61**, o452–o456.
Portilla, J., Quiroga, J., Cobo, J., Low, J. N. & Glidewell, C. (2006). *Acta Cryst.* C**62**, o186–o189.
Portilla, J., Quiroga, J., Cobo, J., Low, J. N. & Glidewell, C. (2007). *Acta Cryst.* C**63**, o26–o28.
Portilla, J., Quiroga, J., Torre, J. M. de la, Cobo, J., Low, J. N. & Glidewell, C. (2006). *Acta Cryst.* C**62**, o521–o524.
Quesada, A., Marchal, A., Melguizo, M., Low, J. N. & Glidewell, C. (2004). *Acta Cryst.* B**60**, 76–89.
Rice, K., Co, E. W., Kim, M. H., Bannen, L. C., Bussenius, J., Le, D., Tsuhako, A. L., Nuss, J., Wang, Y., Xu, W. & Klein, R. R. (2006). Patent numbers WO2006071819-A1, EP1848719-A1, AU2005322085-A1, JP2008525526-W; *Chem. Abs.* **145**, 124611.
Riddell, F. & Rogerson, M. (1996). *J. Chem. Soc. Perkin Trans. 2*, pp. 493–504.
Riddell, F. & Rogerson, M. (1997). *J. Chem. Soc. Perkin Trans. 2*, pp. 249–255.
Seela, F., Jawalekar, A. M., Budow, S. & Eickmeier, H. (2005). *Acta Cryst.* C**61**, o562–o564.
Seela, F., Sirivolu, V. R., He, J. & Eickmeier, H. (2005). *Acta Cryst.* C**61**, o67–o69.
Seela, F., Zhang, Y., Xu, K. & Eickmeier, H. (2005). *Acta Cryst.* C**61**, o60–o62.
Seela, F., Zulauf, M., Reuter, H. & Kastner, G. (1999). *Acta Cryst.* C**55**, 1947–1950.
Seela, F., Zulauf, M., Reuter, H. & Kastner, G. (2000). *Acta Cryst.* C**56**, 489–491.
Senga, K., Novinson, T., Wilson, H. R. & Robins, R. K. (1981). *J. Med. Chem.* **24**, 610–613.
Sheldrick, G. M. (2003). *SADABS*, Version 2.10. University of Göttingen, Germany.
Sheldrick, G. M. (2008). *Acta Cryst.* A**64**, 112–122.
Spek, A. L. (2003). *J. Appl. Cryst.* **36**, 7–13.
Thallypally, P. K. & Nangia, A. (2001). *CrystEngComm*, **3**, 114–119.
Wardell, J. L., Low, J. N., Skakle, J. M. S. & Glidewell, C. (2006). *Acta Cryst.* B**62**, 931–943.
Wardell, S. M. S. V., de Souza, M. V. N., Wardell, J. L., Low, J. N. & Glidewell, C. (2007). *Acta Cryst.* B**63**, 879–895.
Wilson, A. J. C. (1976). *Acta Cryst.* A**32**, 994–996.
Zhang, X., Budow, S., Leonard, P., Eickmeier, H. & Seela, F. (2006). *Acta Cryst.* C**62**, o79–o81.